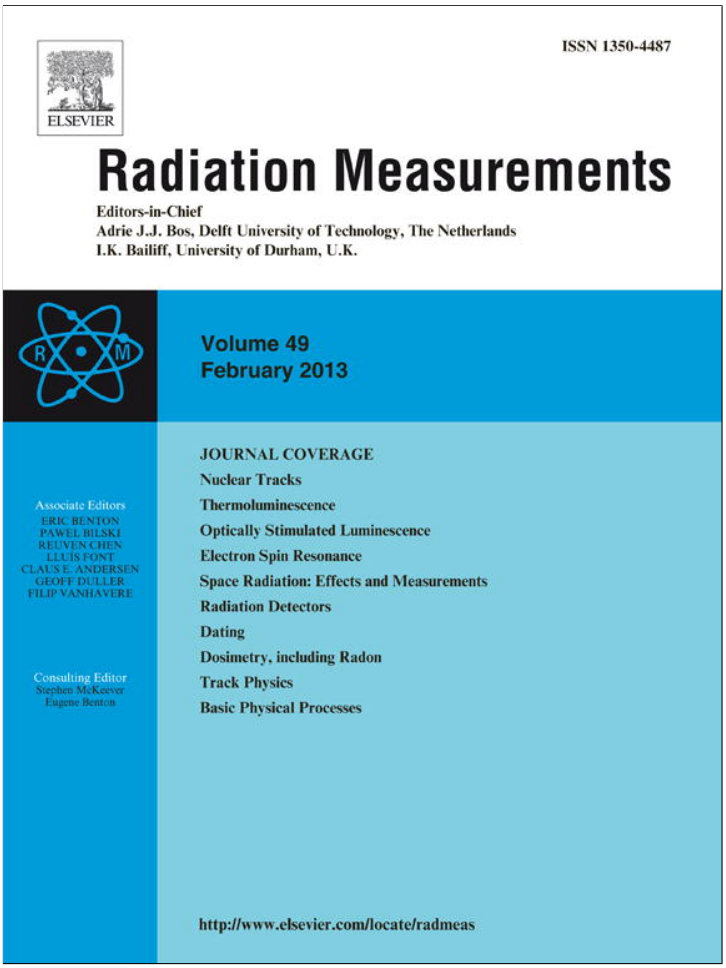

Radiation Measurements 49 (2013) 73–81

Contents lists available at SciVerse ScienceDirect

Radiation Measurements

journal homepage: www.elsevier.com/locate/radmeas

Anomalous fading of OSL signals originating from very deep traps in Durango apatite

G. Kitis [a,*], G.S. Polymeris [b,c], V. Pagonis [d], N.C. Tsirliganis [c]

[a] Aristotle University of Thessaloniki, Nuclear Physics Laboratory, 54124 Thessaloniki, Greece
[b] Aristotle University of Thessaloniki, Solid State Physics Section, 54124 Thessaloniki, Greece
[c] Laboratory of Radiation Applications and Archaeological Dating, Department of Archaeometry and Physicochemical Measurements, "Athena", Tsimiski 58, GR-67 100 Xanthi, Greece
[d] McDaniel College, Physics Department, Westminster, MD 21157, USA

HIGHLIGHTS

- ► Anomalous fading of OSL from very deep traps is much slower than of conventional OSL in Durango apatite.
- ► Blue light and IR stimulation are followed by a strong DOSL signal called relaxation signal.
- ► The Anomalous fading of the relaxation signal is similar to that of TL and OSL signals.
- ► The data supports the correlation of relaxation signal with electron lifetime in conduction band.

ARTICLE INFO

Article history:
Received 31 May 2012
Received in revised form
8 November 2012
Accepted 10 November 2012

Keywords:
Thermoluminescence
Anomalous fading
Apatite
Optically stimulated luminescence
Luminescence dating

ABSTRACT

Athermal or anomalous fading (AF) is one of the most serious problems in thermoluminescence (TL) and optically stimulated luminescence (OSL) dating. Several possible ways have been suggested for choosing a non-fading signal in feldspars, including high temperature thermal preconditioning of the samples. The aim of the present work is to search for stable OSL signals in Durango apatite, a material which exhibits very strong AF effects, by focusing on the existence of optically sensitive very deep traps (VDT). These are traps which are responsible for TL peaks above 500 °C. Two experimental protocols are used to establish the optimal stimulation temperature for these OSL signals from VDT, in order to estimate the activation energy for these signals, and to study their AF properties. It is found that the OSL signals from VDT are more stable than conventional signals from traps responsible for TL peaks below 500 °C, and that they exhibit smaller anomalous fading effects. A new luminescence signal is reported in this material, consisting of a long-lived luminescence decay, observed after the end of short 1 s optical pulses. This new relaxation signal is observed after both blue light stimulation and infrared stimulation of the sample.

1. Introduction

The success of thermoluminescence (TL) and optically stimulated luminescence (OSL) as passive dosimetric tools is based on the existence of energy levels with very long lifetime in inorganic materials. These levels are capable of storing the radiation dose delivered to them by ionizing irradiations originating in naturally occurring radioactive isotopes and cosmic radiation, as well as from laboratory irradiation sources. From the TL and OSL point of view, all inorganic nature is a huge passive dosimeter, giving rise to many dosimetry and dating applications.

One of the advantages of TL and OSL dating is the widespread existence of inorganic materials which act as natural dosimeters. Theoretically, the upper age limit of dating applications is set by a combination of the lifetime and the saturation dose of energy levels. Unfortunately, in some inorganic materials a rapid fading of the luminescence signals is observed experimentally within short times after irradiation, instead of within the long lifetimes predicted by standard kinetic models. This rapid fading process has been termed athermal or anomalous fading (AF), and is one of the most serious problems in TL and OSL dating (Wintle, 1973, 1977).

Extensive experimental and modeling work has been focused on luminescence signals from feldspars, since they exhibit an extended dose range and their luminescence signals saturate at higher doses than quartz. Early attempts to circumvent the AF problem were made by Sutton and Zimmerman (1978) and Templer (1985) and

* Corresponding author.
E-mail address: gkitis@auth.gr (G. Kitis).

1350-4487/$ – see front matter © 2012 Elsevier Ltd. All rights reserved.
http://dx.doi.org/10.1016/j.radmeas.2012.11.011

explanations of the AF effect have been based on various proposed models, such as the tunneling model (Visocekas et al., 1976; Visocekas and Geoffroy, 1977; Visocekas, 1985), the localized transition model (Templer, 1986; Tyler and McKeever, 1988) and a model based on competition with radiationless transitions (Chen, 2000). The most accepted current explanations of AF are based on quantum mechanical tunneling from the ground state of the trap (Poolton et al., 2002a, 2002b; Li and Li, 2008; Kars et al., 2008; Larsen et al., 2009). Based on the observation that AF can be described by a power-law decay, corrections for the dose underestimation arising from this fading effect have been attempted (Huntley and Lamothe, 2001; Auclair et al., 2003; Lamothe et al., 2003; Huntley, 2006).

In recent years several investigations have attempted to overcome the problem of anomalous fading, by searching for new luminescence signals which might exhibit smaller AF effects. Recent extensive experimental work by Jain and Ankjrgaard (2011) elucidated the complexity of the luminescence processes in feldspars. Specifically these authors compared the blue emissions from feldspar under both resonant IR and non-resonant green excitations. They also examined elevated-temperature IRSL which has shown more promise as a luminescence signal than room temperature IRSL (Jain and Singhvi, 2001; Thomsen et al., 2008). The results of Jain and Ankjrgaard (2011) were interpreted within the framework of a model containing several possible recombination routes, namely (a) via the ground state and the excited state of the trap, (b) via the band tail states and (c) through the conduction band (Jain and Ankjrgaard, 2011) (their Fig. 3). These authors suggested three possible ways of choosing a non-fading signal in feldspars, as follows. Firstly, high temperature thermal preconditioning can lead to more stable traps; a preheat of 350 °C was suggested for isolating a luminescence signal that would exhibit smaller AF effects. Secondly, it was suggested that an elevated temperature IR bleach can lead to similar results as the thermal preconditioning of the sample. Thirdly, time-resolved IRSL (TR-IRSL) signals were shown to have promising non-fading properties.

Durango apatite is a natural material which is known to exhibit strong anomalous fading effects. Previous work by Kitis et al. (1991) has shown that all traps responsible for TL peaks up to 500 °C suffer from strong anomalous fading. These authors studied AF effects for a variety of experimental conditions and sample preconditioning. Specifically they used different grain sizes, annealing temperatures between 500 and 1000 °C, radiation predoses between 500 Gy and 2 kGy, and irradiation temperatures between liquid nitrogen temperature and 200 °C. It was found that the AF phenomenon was present under all these diverse experimental conditions, and that the fading rate was affected only somewhat under some of these experimental conditions. In later work, Polymeris et al. (2006) and Tsirliganis et al. (2006) carried out a comparative study of AF effects of TL and OSL signals in this material, and investigated the TL, blue stimulated luminescence (BSL) and infrared stimulated luminescence (IRSL) signals. All of these signals exhibited strong anomalous fading, and contained two components termed fast and slow. The AF properties of the remnant TL, BSL and IRSL signals as a function of the storage time were fitted using equations from the tunneling model, and the fading rate (expressed as the percentage per decade, g) was evaluated. The g values of the BSL and IRSL signals were larger than the corresponding value for the TL signal, while the AF rate of the fast component of BSL and IRSL was practically the same. However, the AF rate of the slow component of IRSL was found to be stronger than the AF rate for the BSL signal by a factor of 2. Kitis et al. (2006) studied the effect of varying the heating rate during a TL measurement on the AF properties of the same natural crystal. They found that the integrated TL signal increased dramatically with increasing heating rate, in disagreement with standard kinetic models of TL in which the integrated TL signal stays the same, or decreases due to thermal quenching effects. An important result from this study was the apparent decrease of the AF with increasing heating rate. Tsirliganis et al. (2007) investigated the dependence of the AF of TL/OSL signals in this material on the occupancy of the recombination sites. These authors found that a reduction of the available recombination centers leads to a corresponding reduction of the AF rate. Furthermore, the experimentally observed changes in the rate of anomalous fading agreed with calculations based on a simple tunneling model.

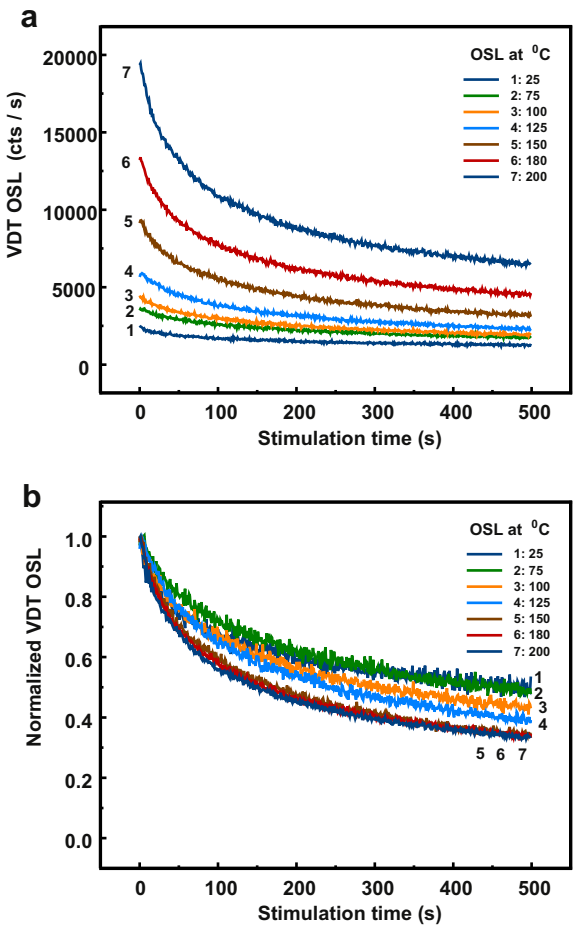

Fig. 1. (a): CW-OSL signal emanating from VDT (very deep traps) measured in the framework of the first protocol (step 3), for various stimulation temperatures. The same curves are also presented in (b) normalized over the maximum initial intensity in order to present possible changes taking place in the shape of the CW-OSL curves.

The aim of the present work is to search for stable OSL signals in this material, by focusing on the existence of optically sensitive very deep traps (VDT). These are traps which are responsible for TL peaks above 500 °C, similar to the VDT recently studied in quartz (Kitis et al., 2010). The VDT are very difficult to observe using luminescence techniques, mostly because of the thermal quenching of the luminescence centers. Secondly, at such high temperatures the interference of high infrared background makes such TL measurements up to 900 °C quite problematic. Furthermore, since these traps have a large thermal trap depth, they are not accessible by TL using commercially available TL readers. Apart from this, conventional OSL using visible stimulation light sources of various wavelengths at ambient temperatures is also incapable of assessing such deep traps, as the photo-ionization cross section of these traps is expected to be very low at ambient temperatures. For all the reasons stated above and in conjunction with instrumental limitations imposed for the commercially available luminescence readers, mostly indirect ways were applied in order to study these deep

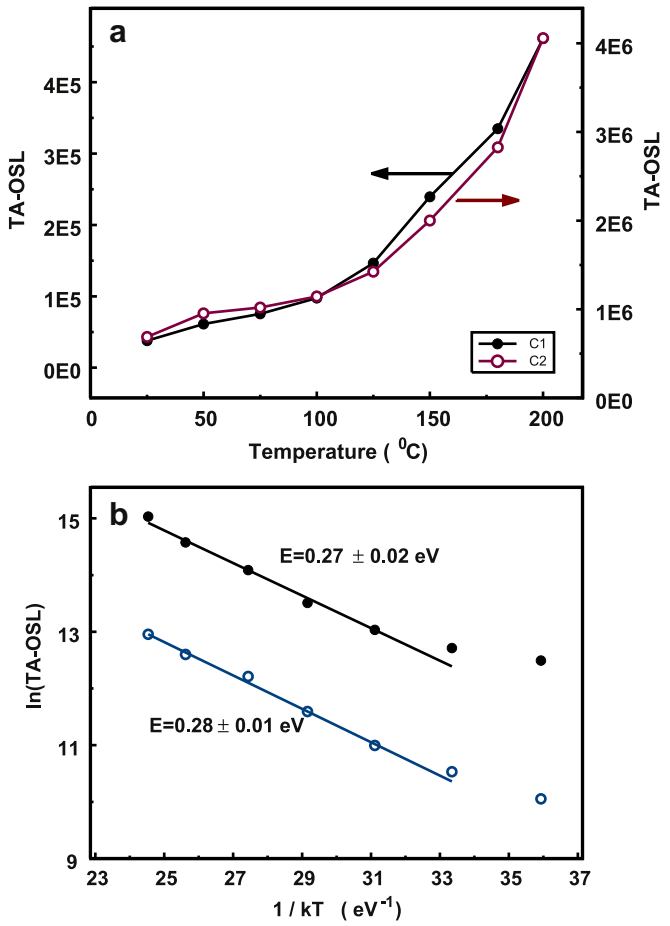

Fig. 2. (a): The TA-OSL of each component in terms of integrated signal, plotted versus stimulation temperature. (b) The corresponding Arrhenius plots are used for evaluating the activation energies of the TA-OSL effect.

traps. Besides TSEE and PTTL, deep traps could be observed in thermally stimulated conductivity (TSC) and TL measurements after irradiation at elevated temperatures. Recently, thermally assisted OSL (TA-OSL) was also shown to be very effective. Especially in the case of Al_2O_3:C, three out of four studies of VDT are conducted by using indirect methods, instead of measuring TL up to 900 °C.

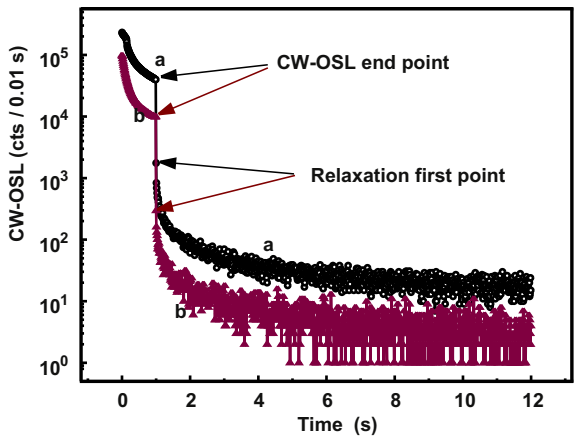

Fig. 3. The OSL decay curves obtained in the framework of the second protocol (step 3). Curve (a) corresponds to a measurement immediately after irradiation, and curve (b) to a measurement after the maximum storage time of 240 min. Curves (a) and (b) consist of two parts, with the first part corresponding to a brief (1 s) blue stimulation which ends at the points shown in the figure. The second part of the signal is the DOSL, not previously reported for this material.

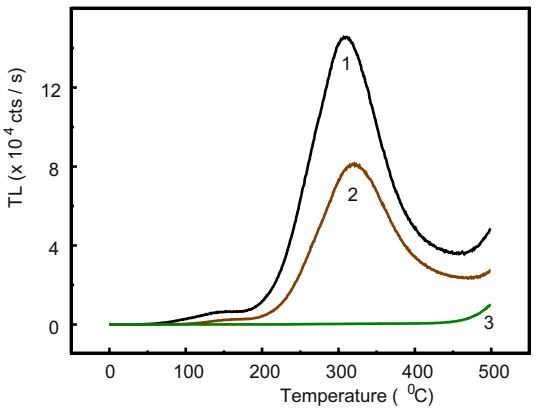

Fig. 4. TL glow curves for storage times of "zero" and 240 min (curves (1) and (2) respectively). Curve 3 corresponds to the residual TL obtained in step 6 of the second protocol.

Polymeris and Kitis (2012) in a new detailed study of the VDT in Al_2O_3:C provide an extended literature review on studies of VDT.

In terms of the three methods suggested by Jain and Ankjrgaard (2011) for choosing a more stable signal, the present study falls into their first category, namely that of thermal preconditioning of the sample.

2. Experimental procedure

2.1. Sample

The sample used in these experiments was a natural crystal of Durango apatite with dimensions of 8 × 4 × 3 mm. The single piece crystal was crushed gently with an agate mortar and grains of dimension 80–140 μm were obtained after sieving. The grains were annealed at 900 °C for 1 h, followed by rapid cooling to room temperature. This annealing treatment is necessary in order to empty all VDT, which may have been filled by the natural irradiation of the material. Previous work has shown that this annealing process does not influence the anomalous fading effect in Durango apatite (Kitis et al., 1991).

Aliquots (sub-samples) with the same mass of 5 mg were attached to stainless steel disks. Each data point reported in this paper was the average of two measurements carried out on two different aliquots/disks.

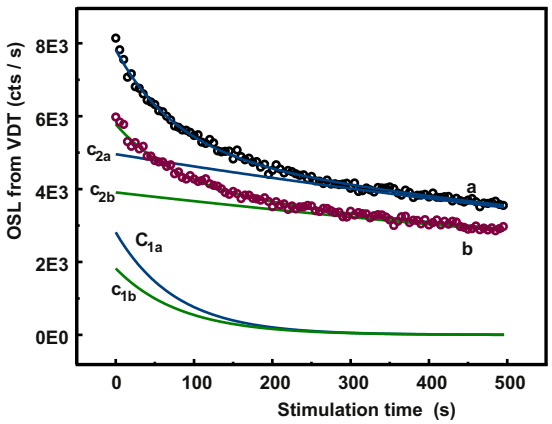

Fig. 5. Analysis of the TA-OSL curves, which are measured in the framework of the second protocol (step 5), by using the sum of two exponentials. Both sets of data were measured at 180 °C. Curve (a) corresponds to a "zero" storage time, and curve (b) to the maximum storage time of 240 min.

2.2. Apparatus and measurement conditions

Both TL and OSL measurements were carried out using a Risø TL/OSL reader (model TL/OSL-DA-15), equipped with a $^{90}Sr/^{90}Y$ beta particle source, delivering a nominal dose rate of 0.075 Gy/s. A 9635QA photomultiplier tube is used for light detection. The stimulation wavelength is 470 nm, delivering at the sample position a maximum power of 40 mW cm^{-2}. The detection optics consisted of a 7.5 mm Hoya U-340 filter ($\lambda_p \sim 340$ nm, FWHM ~ 80 nm). All measurements were performed in a nitrogen atmosphere with a low constant heating rate of 1 °C/s, in order to avoid significant temperature lag, and the samples were heated up to the maximum temperature of 500 °C.

2.3. Experimental protocols

The experimental procedure of the present work uses two protocols. The first protocol is used to find the optimal temperature for measuring the OSL signals from VDT. This protocol is very similar to the one used by Kitis et al. (2010), who measured the OSL signal from VDT in quartz.

- Step 1: The previously annealed aliquot is irradiated with a test dose TD = 15 Gy, in order to populate the traps and centers.
- Step 2: TL measurement up to 500 °C, in order to erase all glow-peaks up to 500 °C.
- Step 3: Blue CW-OSL at T_i for 500 s (T_i = 25, 75, 100, 125, 150, 180 and 200 °C). This represents the CW-OSL signal from VDT, and this step allows a study of this signal at different stimulation temperatures (Fig. 1(a)).
- Step 4: TL measurement up to 500 °C. The residual TL signal will be compared to the TL signal obtained in step 2 of the protocol. This step also checks whether a phototransferred signal is created by the blue light CW-OSL stimulation used in step 3.
- Step 5: Repeat steps 1–4 for a new aliquot and for a new stimulation temperature T_i.

There are two goals for this first protocol. Firstly, to establish the optimum stimulation temperature for measuring the OSL signal from VDT. This optimal temperature will be used in the second protocol. Secondly, to evaluate the thermal activation energy of the OSL signals from VDT, in analogy to similar measurements carried out in quartz (Kitis et al., 2010). Data presented in Fig. 2 are discussed in Section 3.1.

A second experimental protocol is used to study the anomalous fading effect for two types of CW-OSL signals, those originating from traps responsible for the TL signal up to 500 °C, and also for the CW-OSL signal originating in VDT. The steps in this second protocol are as follows:

- Step 1: The aliquot is irradiated with a test dose, TD = 15 Gy. The purpose of this step is to populate the traps and centers in the annealed aliquots.
- Step 2: Store the sample in the dark and at room temperature, for nine storage times t_i = 0, 5, 10, 30, 45, 60, 90, 120, 240 min.
- Step 3: Blue CW-OSL at room temperature for 1 s, followed by measurement of the OSL signal for an additional 11 s after the end of the 1 s stimulation. The purpose of this step is described below. Typical results from this step of the protocol are shown in Fig. 3.
- Step 4: TL measurement up 500 °C, in order to empty all traps up to this temperature. This step also prepares the sample for the next step in the protocol, in which the OSL signal from VDT is measured.
- Step 5: Blue CW-OSL at T_{CW} for 500 s. This step measures the CW-OSL from VDT. The optimal temperature of T_{CW} would have been determined from the results of the first protocol.
- Step 6: TL measurement up to 500 °C. The intensity of this residual TL signal will be compared to the TL signal obtained in step 4 of the protocol. This step also checks whether a phototransferred signal is created by the blue light stimulation used in step 5.
- Step 7: Repeat steps 1–6 for a new aliquot and for a new storage time t_i.

The aims of step 3 in this second protocol are twofold, namely:

1. To obtain the CW-OSL signal as a function of the storage time, in order to reproduce previous detailed measurements of the anomalous fading effect by Polymeris et al. (2006). The anomalous fading properties of this brief (1 s) CW-OSL signal will be compared with those of the OSL signal from VDT, which is measured in step 5 of the protocol.
2. To study the properties of the relaxation signal measured during the 11 s time interval which follows the brief 1 s optical stimulation of the sample.

Two additional notes are necessary for the experimental procedure in steps 2 and 3 of the second protocol. In step 2 the exact zero storage time is not possible, because there is always a minimum time elapsed between the end of the irradiation and TL or OSL measurement. In the TL–OSL reader used this time is set equal to 120 s. Consequently, this time is added to the storage time sequence of step 2. Therefore, instead of zero time storage the term "zero" storage will be used hereafter in the text.

Step 3 mimics the technique of pulsed optical stimulated luminescence (POSL), in which a short pulse of optical stimulation is followed by a relaxation period in which the stimulating source is turned off. This 11 s relaxation signal provides valuable information on the slower relaxation processes which take place after the end of optical stimulation.

Step 4 is crucial because it is necessary for the experiment to empty all electron traps thermally activated below 500 °C. For this reason the very low heating rate of 1 °C/s was used in all cases of TL readout. The goal of step 5 in the second protocol is to study the anomalous fading effects for blue CW-OSL signals from VDT, measured at a stimulation temperature of T_{CW}.

The final TL readout in step 6 is crucial. Based on kinetic theory it is assumed that if the stimulation light can liberate electrons from VDT they will have two main pathways. First, to recombine giving rise to a direct single step OSL signal and second to be retrapped in shallower traps existing between the OSL measuring temperature T_{CW} and the 500 °C. During the optical stimulation the retrapped electrons of the second pathway have two alternatives. The first is to be stimulated again giving rise to a two-step OSL from VDT and the second is to survive from the stimulation and be observed as a phototransferred TL signal (also observed in step 4 of protocol 1). Therefore, this step will show if some phototransfer signal can survive as a TL signal according to the second alternative.

3. Results and discussion

3.1. Results from the first protocol: OSL from VDT

As mentioned previously, the main goal of the first protocol is to obtain the optimal stimulation temperature for CW-OSL signals from VDT in this material. The CW-OSL decay curves measured in step 3 of the first protocol are shown in Fig. 1(a), while Fig. 1(b) shows the same data as Fig. 1(a), normalized over the first data

point. The shape of the CW-OSL curves changes between stimulation temperatures of 25 and 125 °C (curves 1–4), while it remains the same at the higher stimulation temperature range of 150–250 °C (curves 5–7).

Each of the curves in Fig. 1 was analyzed empirically into two components, termed here C_1 and C_2, by using the sum of two exponentials as follows:

$$I(t) = C_1 + C_2 = A_1 \exp\left(-\frac{t}{B_1}\right) + A_2 \exp\left(-\frac{t}{B_2}\right). \quad (1)$$

Where A_1, A_2 are the intensities of the components at $t = 0$ and B_1, B_2 the mean lifetimes.

The main interest from the analysis using Eq. (1) is to evaluate the total integrals of components C_1 and C_2. However, the analysis gives also the values of the mean lifetimes B_1 and B_2. Although, there is a small increasing trend from $T_{CW} = 25$ °C up to 200 °C the overall increase is less than 10% for B_1 and 16% for B_2. For this reason only the mean values will be given which are $B_1 = 66.7 \pm 7$ s and $B_2 = 1250 \pm 200$ s. A similar analysis is performed in Subsection 3.3 where further examples of analyzed curves are given and discussed.

From Figs. 1 and 2(a) it is observed that the magnitude of the OSL signal increases exponentially as the stimulation temperature increases. This observation has also been well documented for quartz samples (Bøtter-Jensen et al., 2003; Kitis et al., 2010) and Al_2O_3:C (Polymeris and Kitis, 2012).

Fig. 2(a) shows the behavior of the integrated signal of the components C_1 and C_2 obtained by the analysis of the data in Fig. 1(a) as a function of the stimulation temperature. The integrated signal of each component increases rapidly as a function of the stimulation temperature, a phenomenon previously termed thermally assisted OSL (TA-OSL). The activation energy of this TA-OSL signal can be estimated from an Arrhenius plot in which the natural logarithm of the integrated signal is plotted as a function of the inverse temperature ($1/kT$). This is shown in Fig. 2(b) in which the contribution of the OSL at room temperature was considered as the maximum possible background signal and was subtracted from the OSL signals at higher temperatures. The slope of the linear parts of Fig. 2(b) are found to be $E = 0.28 \pm 0.01$ eV for component C_1 and $E = 0.27 \pm 0.02$ eV for the component C_2.

From the data in Fig. 2(a), the temperature of 200 °C gives the maximum CW-OSL signal. However, the temperature of 180 °C, which gives also an intense CW-OSL signal was chosen as the optimum stimulation temperature. This optimal stimulation temperature was used throughout the second protocol.

The intensity of the residual TL signal measured in step 4 of the first protocol was about 1% of the TL signal obtained in step 2 of the protocol. This indicates that the TL readout applied in step 2 erased all glow-peaks up to 500 °C. Furthermore, the very small residual TL signal in step 4 indicates that there is negligible phototransferred signal created by the blue light stimulation used in step 3 of the first protocol.

3.2. The delayed OSL (DOSL) and TL glow curves

Typical results obtained in step 3 of the second protocol are shown in Fig. 3. Curve (a) corresponds to a measurement immediately after irradiation ("zero" storage time) and curve (b) to a measurement after the maximum storage time of 240 min. Each one of the curves (a) and (b) consists of two parts. The first part corresponds to 1 s of blue stimulation, which ends at the points indicated by the arrows in the figure. Presumably, even though the blue light stimulation ceases at these points, the charge carriers in the material continue to participate in the luminescence process giving rise to the second part of the curve. This second part of the signal has the characteristics of the delayed OSL (DOSL) discussed by Bøtter-Jensen et al. (2003) (and references therein). A similar signal was also reported by Jaek et al. (1999) which was termed by them OSL afterglow (OSLA) and was attributed to phosphorescence from shallow traps filled by the optical stimulation.

As can be seen in Fig. 3, the CW-OSL signal decreases rather quickly within the brief 1 s optical stimulation, by almost an order of magnitude. The subsequent DOSL signal shows also a fast initial decrease within the first 0.1 s, followed by a slower decrease over the next 11 s. The AF properties of these two signals are summarized in Fig. 6, and are discussed in subsequent sections.

Fig. 4 shows the TL glow curve measured in step 4 of the second protocol. Curve (1) corresponds to a "zero" storage time, while curve (b) to the maximum storage time of 240 min. Fig. 4 shows that this remnant TL signal decays by almost 50% over the range of storage times used in the experiment. It is also noted that the maximum of the "240 min" glow curve is shifted towards higher temperatures. These TL glow curves contain peaks at approximately 150 °C and 300 °C. Similar TL glow curves were analyzed previously by Polymeris et al. (2006), by using a second order kinetics model.

Curve (3) in Fig. 4 corresponds to the residual TL obtained in step 6 of the second protocol. The integrated signal of curve (3) is of the same intensity for all storage times used, and is equal to 1% of the total integrated signal of curve (1), and to 3% of the total integrated signal of curve (2). These results indicate that the TL readout applied in step 4 of the protocol successfully erased all glow-peaks up to 500 °C. Furthermore, the smallness of the residual TL signal in curve (3) indicates there is no evidence of a phototransfer signal caused by the blue light stimulation used in step 5 of the second protocol.

3.3. Results from the second protocol: OSL from VDT at 180 °C

Two typical examples of CW-OSL curves from VDT obtained in step 5 of the second protocol, are shown in Fig. 5. These CW-OSL curves were measured at the same optimal stimulation temperature of 180 °C. Curve (a) in this figure corresponds to "zero" storage time (i.e. immediately after the end of irradiation), while curve (b) corresponds to the longest storage time of 240 min. A total of $9 \times 2 = 18$ CW-OSL curves was measured; these correspond to the 9 storage times, and to the two aliquot used for each of these storage times. Each one of these 18 curves was analyzed empirically into

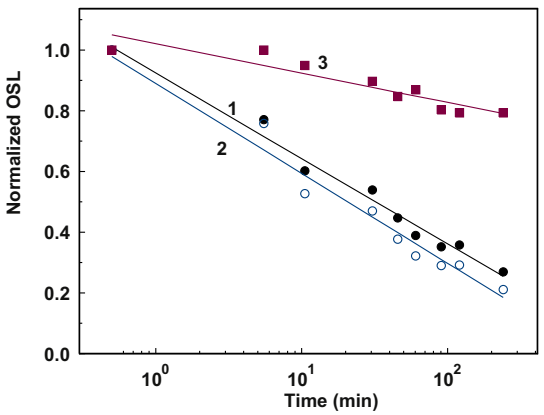

Fig. 6. Remnant OSL signal normalized over the its value at "zero" storage time, as a function of storage time, in terms of the OSL signal during the 1 s blue stimulation (curve (1)) as well as the total integral of the DOSL signal (curve (2)). Curve (3) corresponds to the TA-OSL signal from VDT. The three sets of data are fitted using Eq. (2).

two components, by using the sum of two exponentials given by Eq. (1).

In typical kinetic models for luminescence processes, the exponential terms in Eq. (1) would represent first order kinetics with negligible retrapping. These two components as well as their sum, are shown as solid lines in Fig. 4, for curves (a) and (b). The resulting value of the constant B_1 is 76.9 ± 8 s and of the constant B_2 is 1492 ± 250 s. These values are in good agreement with the corresponding values obtained in Section 3.1 for the case of OSL from VDT as a function of OSL measuring temperature.

The TL–OSL signals monitored during an anomalous fading experiment are the remnant TL/OSL, i.e. they represent the signals remaining after various times have elapsed from the end of irradiation. These remnant signals are defined as the ratio r of the TL/OSL signal remaining after storage time t, to the TL/OSL measured at a reference time t_0 after the end of the irradiation (Polymeris et al., 2006). Specifically one writes:

$$r = 1 - K \cdot \ln \frac{t}{t_0}, \tag{2}$$

where K is a dimensionless constant. In practice, one fits the data to this equation by treating K and t_0 as adjustable fitting parameters. A quantity commonly used to express the rate of anomalous fading, is the fading rate in percentage per decade, g (Aitken, 1985). This quantity is related to the constant K in Eq. (2) by the expression:

$$g = 230.2\ \mathrm{K}. \tag{3}$$

Fig. 6 shows the remnant OSL signal normalized over the value at "zero" storage time, as a function of storage time t, for three different signals. Curve (1) in this figure corresponds to the integrated CW-OSL signal measured during the 1 s of blue stimulation shown in Fig. 3. This signal originates in traps corresponding to TL peaks below 500 °C, and the resulting value of K from the slope of curve (1) is $K = 0.122 \pm 0.005$. This value of K gives a percentage per decade $g = 28.1 \pm 1.2$, in close agreement with the anomalous fading value of $g = 28.4$ found by Polymeris et al. (2006) using blue light OSL. It is concluded that the short (1 s) OSL signal shown in Fig. 3 is consistent with the previous work by Polymeris et al. (2006).

Curve (3) of Fig. 6 corresponds to the fading properties of the integrated OSL signal from VDT, which was obtained in step 5 of the second protocol. The resulting value of the fading parameter is $K = 0.055 \pm 0.002$, which gives a percentage per decade $g = 12.7 \pm 0.5$. This value is lower by a factor of 2.3 than the value of $g = 28.1 \pm 1.2$ obtained above for the OSL signal originating from traps corresponding to TL peaks below 500 °C. From a practical point of view, this is the most important result from this paper, indicating that thermal pretreatment of the apatite samples by heating to 500 °C, causes blue light to access optically sensitive VDT in this material. The resulting CW-OSL signal from VDT is clearly more stable, showing much smaller anomalous fading over time.

Curve (2) of Fig. 6 describes the anomalous fading properties of the DOSL signals reported in this paper, and these are discussed in the next section.

3.4. Analysis of the DOSL signals

The DOSL signals shown in Fig. 3 have not previously reported for this material. Their long duration (for more than 11 s) at room temperature is rather surprising, and their origin is unknown. The DOSL signals obtained for the 2 × 9 storage times were analyzed on an empirical basis by using the sum of three exponential components of the form:

$$I(t) = C_1 + C_2 + C_3 = A_1 \exp\left(-\frac{t}{B_1}\right) + A_2 \exp\left(-\frac{t}{B_2}\right) + A_3 \exp\left(-\frac{t}{B_3}\right). \tag{4}$$

Where A_1, A_2, A_3 are the intensities at $t = 0$ and B_1, B_2, B_3 are the mean lifetimes. As previously mentioned, these components could represent first order kinetics processes with negligible retrapping. An example of this type of analysis is shown in Fig. 7. The mean lifetime of each component resulting from the 9 × 2 = 18 analyzed DOSL curves for components C_1, C_2 and C_3 are: $B_1 = 0.023 \pm 0.0001$ s, $B_2 = 0.4 \pm 0.06$ s and $B_3 = 3.3 \pm 0.5$ s. A fourth "very fast" exponential component may be present, but its contribution is restricted to within the first two points of the DOSL curves of Fig. 3. The resolution of the experimental data with the sampling interval of 0.01 s does not allow for accurate determination of this very fast DOSL component.

Fig. 8 shows the anomalous fading results of the three components of the DOSL part shown in Fig. 3. All three exponential components show the same anomalous fading behavior, and the mean value of K was found to be $K = 0.130 \pm 0.006$. According to Eq. (3) this value of K corresponds to a percentage per decade $g = 29.9 \pm 1.4$, in close agreement with the value of $g = 28.4$ found previously by Polymeris et al. (2006) and Tsirliganis et al. (2006).

These DOSL signals are found to be at least an order of magnitude larger than the background signal measured at room temperature, which was estimated to be 54 ± 8 counts/s, or 0.54 ± 0.08 counts/0.01 s (for the sampling time interval of 0.01 s used in Fig. 3). Therefore, this background signal contributes very little to the DOSL decay curves obtained in this experiment, and is not visible in the experimental data shown in Fig. 3. In terms of the overall integrated signal, this background represents about 1% of the total integral for the "zero" storage time, and increases up to 5% for the longest storage time of 240 min.

3.5. Investigation of the origin of the DOSL signal

Several possible explanations for the DOSL signal are possible. Firstly, it could be due to the presence of shallow traps in this material, which can be thermally unstable at room temperature. Charge carriers from these traps could be thermally excited into the conduction band after the end of the irradiation, and would cause a long-lived phosphorescence signal at room temperature. A second alternative explanation is that this DOSL signal originates from charge carriers which were excited into the conduction band during the short optical stimulation, and which undergo a slow

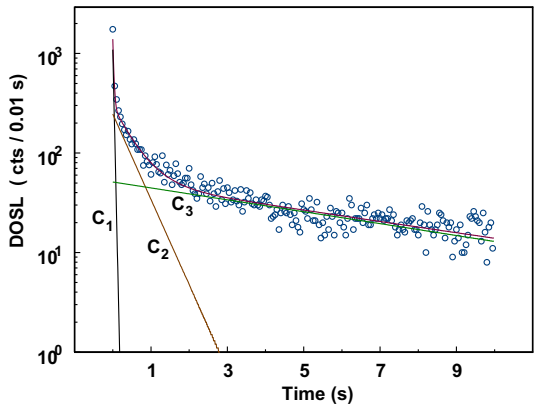

Fig. 7. De-convolution analysis of the DOSL signal of Fig. 3, by using the sum of three exponential components.

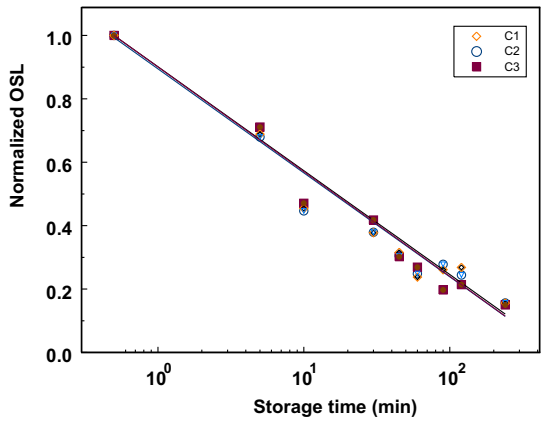

Fig. 8. Component resolved remnant DOSL versus storage time. The data set of each component was fitted by using Eq. (2). All three lines coincide.

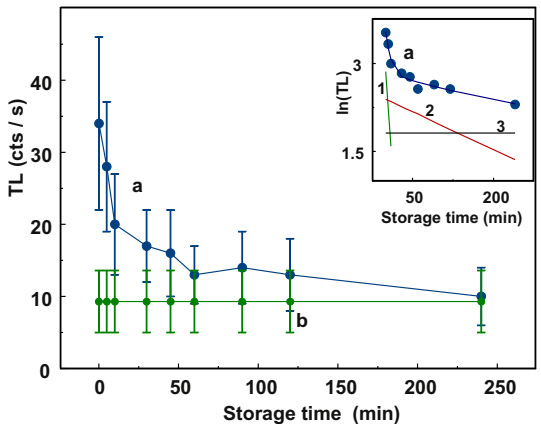

Fig. 10. Phosphorescence signal at room temperature as a function of the storage time, obtained from carrying out an analysis similar to Fig. 9. The background signal from an empty stainless steel disk is also shown as a constant horizontal line. Inset: The same plot in semi-log axis, de-convolved into two components and the background.

DOSL process into the luminescence center after the end of the pulse. A third possible explanation is that this long-lived DOSL signal originates from charges which were excited into the band tail states which are known to exist in feldspar materials (Jain and Ankjrgaard (2011) and references therein).

Several important questions can be raised in connection with these DOSL signals and their properties: (a) Are these signals due to phosphorescence of shallow traps? (b) Can these DOSL signals be observed using a different stimulation wavelength than the blue light used in Fig. 3? (c) Is the shape of these signals truly the sum of exponentials?

The experimental TL data helps rule out the first possible explanation, namely that these are "phosphorescence" signals due to shallow traps, which are thermally unstable at room temperature. Fig. 9 shows the TL signal up to 175 °C, as measured in step 4 of the second protocol. The two curves shown correspond to the TL glow curves measured after a "zero" storage time, and the maximum storage time of 240 min. By taking the average of the first 25 channels in these glow curves, we estimate the "phosphorescence signal" measured at room temperature for these two storage times. By repeating this process at different storage times, Fig. 10 is obtained, which shows the phosphorescence at room temperature as a function of the storage time. The inset shows its analysis using two components, lines (1) and (2), plus line (3) which is the background curve (b). The corresponding values of the lifetimes are 7.8 ± 1.2 min and 238 ± 20 min for the components (1) and (2). These values are much higher that the lifetimes of the relaxation signal obtained in Section 3.4. Furthermore, the magnitude of this "phosphorescence signal" is found to be about 50 times smaller than the DOSL signal shown in Fig. 3. It is concluded that the DOSL signal reported in this paper does not represent "phosphorescence" from shallow traps, but is indeed the results of a charge relaxation process in this material.

In a separate experiment, the nature of the DOSL signal was investigated by using a short IR pulse, instead of the short blue-light pulse used previously. Fig. 11 shows the result of using a short (1 s) IR excitation pulse. The inset shows a detail of the DOSL signal up to 4 s of relaxation time. As seen by comparing this figure with Fig. 3, a similar type of DOSL signal is obtained using IR instead of blue light excitation. However, the fast decaying part of this IRSL-induced DOSL signal in Fig. 11 is about an order of magnitude smaller than the corresponding decay part of the blue-light DOSL signal shown in Fig. 3. The question if the DOSL signal is due to shallow phosphorescence traps can not be answered unambiguously. However, the fact that the intensity of the DOSL signal (in cts/0.01 s) in Fig. 11 is higher than the phosphorescence intensity (in cts/s) in Figs. 9 and 10 is a good indication that it is not phosphorescence.

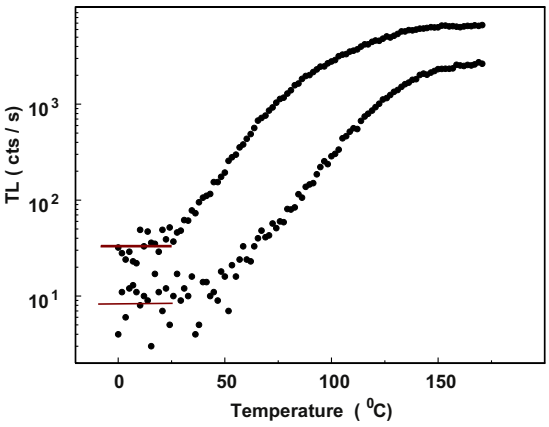

Fig. 9. A detail of Fig. 4 presenting the TL glow curves corresponding to "zero" and 240 min storage time, up to a temperature of 175 °C. The "phosphorescence signal" is estimated at room temperature by taking the average of the first 25 channels.

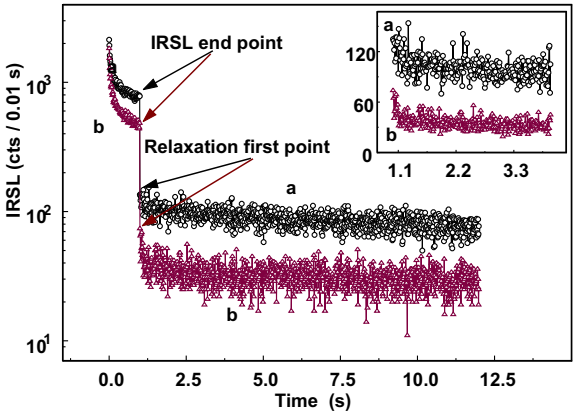

Fig. 11. As in Fig. 3 but using infrared (IR) stimulation. Curve (a) corresponds to a measurement immediately after irradiation, and curve (b) to a measurement after the storage time of 1 min. In order to confirm the presence of a DOSL signal after IR stimulation, a detail of the plot is presented in the inset.

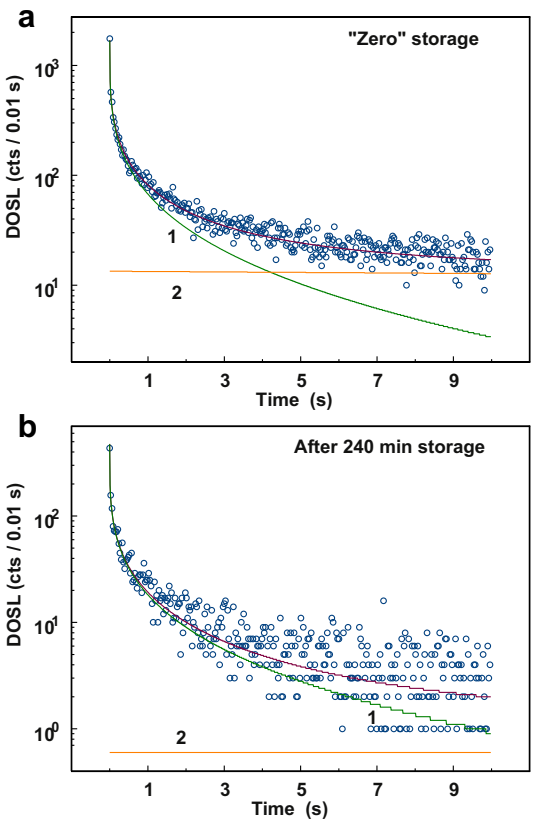

Fig. 12. Alternative analysis of the DOSL signal of Fig. 3, after using a stretched exponential, curve (1), plus a constant, curve (2).

Finally, we investigate the third question posed above, by fitting the DOSL signals with the sum of a stretched exponential plus a constant, along the lines of Pagonis et al. (2012a,b) who investigated in detail the possibility of using the stretched exponential function to fit DOSL data. The equations used in this case is:

$$I(t) = \mathrm{bgd} + I_2 \exp\left(-(t/t_0)^{\beta}\right) \quad (5)$$

where the first term represents a constant background term, t_0, β are the parameters characterizing the stretched exponential term. The results are shown in Fig. 12, where one can see that Eq. (5) gives very good fits to the experimental data. The parameters values obtained were $t_0 = 0.0150 \pm 0.0013$ *s*and $\beta = 0.280 \pm 0.006$.

An alternative way to fit the DOSL decay curves is by using, instead of the stretched exponential of Eq. (5), an expression of the form $1/t^n$ with n a parameter between 0 and 1. The resulting fits are very similar to that of the stretched exponential shown in Fig. 12(a) and (b) with the value of $n = 0.71 \pm 0.03$. This case is very interesting because it is a good indication that the DOSL signal could be related to tunneling recombination. Therefore, further experimental and modeling work is necessary to decide which of the fitting functions is correct.

4. Discussion and conclusions

The results of the present work are highly encouraging, since they show that it is possible to find stable luminescence signals by appropriate preheat treatment of this sample of Durango apatite. The goal of the present work was to search for stable OSL signals, by focusing on the existence of optically sensitive very deep traps. Such traps may be expected to exist in many natural materials, and can be easily accessed and studied using the protocols used in this paper.

The luminescence signal reported in this paper was observed after both blue light and infrared stimulation of the sample. By studying the properties of these DOSL signals using different excitation wavelengths, heat treatments and irradiation conditions, one can extract very useful information about the luminescence pathways. This was shown in the recent extensive study of feldspars by Jain and Ankjrgaard (2011) using time-resolved luminescence experiments in the microseconds time range. The DOSL signals studied here have much longer lifetimes of the order of tens of seconds, and are easier to study experimentally.

The IRSL trap in feldspar is believed to be located at ~2–2.5 eV below the conduction band, and therefore optical stimulation with blue light at a photon energy of 2.63 eV causes a direct transition into the conduction band. However, stimulation with IR light of a wavelength of ~1.4 eV causes resonant electronic transitions from the ground state into the excited state of the trap. Excitation with green LEDs causes electronic transitions of an intermediate nature, between blue and IR excitation energies. It is also believed that a continuum of thermal excitations can take place from the bottom edge of the band tail states, into the excited state of the trap, and eventually into the conduction band. Jain and Ankjrgaard (2011) concluded that electrons from the excited state can either recombine with holes directly by tunneling, or they may be involved in band tail transport through the crystal.

The results of these and other recent experimental studies (Poolton et al., 2009; Thomsen et al., 2011), suggested that the luminescence production mechanism in feldspars depends critically on the distance between the electron and the hole traps in these materials. This distance seems to be one of the more important elements in determining the shape of luminescence signals from these materials. Recent modeling work by Pagonis et al. (2012a,b) also supports the important role played by this parameter in the production of continuous-wave IRSL (CW-IRSL) signals. These authors presented a model which explained the dependence of the shape of CW-IRSL signals on the power of the stimulating light, based on the experimental work of Thomsen et al. (2011). It is possible that Durango apatite may be characterized by a relatively small distance between the electron and the hole traps, leading to the high AF rate exhibited by this material.

On the basis of the experimental observation that the new luminescence signal reported here is observed after both blue light and infrared stimulation, it is hypothesized that this long-lived DOSL signal may originate from charges which were excited into the band tail states. Clearly additional experimental work is necessary to establish the origin and the true nature of these signals.

Further work is required in order to extend the present study to other minerals suffering from anomalous fading, such as apatites of other type and origin but mostly to feldspars. The VDT OSL signal seems to be quite promising for establishing single aliquot dating protocols since it lacks the anomalous fading effect.

References

Aitken, M.J., 1985. Thermoluminescence Dating. Academic Press. Appendix F.
Auclair, A., Lamothe, M., Huot, S., 2003. Measurement of anomalous fading for feldspar IRSL using SAR. Radiat. Meas. 37, 487–492.
Bøtter-Jensen, L., McKeever, S.W.S., Wintle, A.G., 2003. Optically Stimulated Luminescence Dosimetry. Elsevier, Amsterdam.
Chen, R., 2000. Apparent anomalous fading of thermoluminescence associated with competition with radiationless transitions. Radiat. Meas. 32, 505–551.
Huntley, D.J., 2006. An explanation of the power-law decay of luminescence. J. Phys. Cond. Matt. 18, 1359–1365.
Huntley, D.J., Lamothe, M., 2001. Ubiquity of anomalous fading in K-feldspars and the measurement and correction for it in optical dating. Can.J. Earth Sci. 38, 1093–1106.
Jaek, I., Hütt, G., Streltsov, A., 1999. Study of deep traps in alkali feldspars and quartz by the optically stimulated afterglow. Radiat. Prot. Dosim. 84, 467–470.

Jain, M., Singhvi, A.K., 2001. Limits to depletion of blue-green light stimulated luminescence in feldspars: implications for quartz dating. Radiat. Meas. 33, 883–892.
Jain, M., Ankjrgaard, C., 2011. Towards a non-fading signal in feldspars: insight into charge transport and tunnelling from time-resolved optically stimulated luminescence. Radiat. Meas. 46, 292–309.
Kars, R.H., Wallinga, J., Cohen, K.M., 2008. A new approach towards anomalous fading correction for feldspar IRSL dating-tests on samples in field saturation. Radiat. Meas. 43, 786–790.
Kitis, G., Bousbouras, P., Antypas, C., Charalambous, S., 1991. Anomalous fading in apatite. Nucl. Tracks Radiat. Meas. 18, 61–65.
Kitis, G., Polymeris, G.S., Pagonis, V., Tsirliganis, N.C., 2006. Thermoluminescence response and apparent anomalous fading factor of Durango fluorapatite as a function of the heating rate. Phys. Stat. Sol. (a) 203, 3816–3823.
Kitis, G., Kiyak, N.G., Polymeris, G.S., Pagonis, V., 2010. Investigation of OSL signal from very deep traps in unfired and fired quartz samples. Nucl. Instr. Meth. Phys. Res. B 269, 592–598.
Lamothe, M., Auclair, M., Hamzaoui, C., Huot, S., 2003. Towards a prediction of long-term anomalous fading of feldspar IRSL. Radiat. Meas. 37, 493–498.
Larsen, A., Greilich, S., Jain, M., Murray, A.S., 2009. Developing a numerical simulation for fading in feldspar. Radiat. Meas. 44, 467–471.
Li, B., Li, S.H., 2008. Investigations of the dose-dependent anomalous fading rate of feldspar from sediments. J. Phys. D Appl. Phys. 41. http://dx.doi.org/10.1088/0022-3727/41/22/225502 225502
Pagonis, V., Jain, M., Murray, A.S., Ankjrgaard, C., Chen, R., 2012a. Modeling of the shape of infrared stimulated luminescence signals in feldspars. Radiat. Meas. 47, 870–876.
Pagonis, V., Morthekai, P., Singhvi, A.K., Thomas, J., Balaram, V., Kitis, G., Chen, R., 2012b. Time-resolved infrared stimulated luminescence signals in feldspars: analysis based on exponential and stretched exponential functions. J. Lumin. 132, 2330–2340.
Polymeris, G.S., Tsirliganis, N., Loukou, Z., Kitis, G., 2006. A comparative study of anomalous fading effects of TL and OSL signals of Durango apatite. Phys. Stat. Sol. (a) 203, 578–590.
Polymeris, G.S., Kitis, G., 2012. Thermally assisted phototransfer OSL from deep traps in Al_2O_3:C grains exhibiting different TL peak shapes. Appl. Radiat. Isotope 70, 2478–2487.
Poolton, N.R.J., Kars, R.H., Wallinga, J., Bos, A.J.J., 2009. Direct evidence for the participation of band tails and excited-state tunneling in the luminescence of irradiated feldspars. J. Phys. Cond. Matt. 21. art.no. 485505.
Poolton, N.R.J., Wallinga, J., Murray, A.S., Bulur, E., Bøtter-Jensen, L., 2002a. Electrons in feldspar I: on the wave-function of electrons trapped at simple lattice defects. Phys. Chem. Minerals 29, 210–216.
Poolton, N.R.J., Ozanyan, K.B., Wallinga, J., Murray, A.S., Bøtter-Jensen, L., 2002b. Electrons in feldspar II: a consideration of the influence of conduction band-tail states on luminescence processes. Phys. Chem. Minerals 29, 217–225.
Sutton, S., Zimmerman, D.W., 1978. Attempts to circumvent anomalous fading. Ancient TL 3, 10–12.
Templer, R.H., 1985. The removal of anomalous fading in zircon. Nucl. Tracks 10, 531–537.
Templer, R.H., 1986. The localized transition model of anomalous fading. Radiat. Prot. Dosim. 17, 493–497.
Thomsen, K.J., Murray, A.S., Jain, M., Bøtter-Jensen, L., 2008. Laboratory fading rates of various luminescence signals from feldspar-rich sediment extracts. Radiat. Meas. 43, 1474–1486.
Thomsen, K.J., Murray, A.S., Jain, M., 2011. Stability of IRSL signals from sedimentary K-feldspar samples. Geochronometria 38, 1–13.
Tsirliganis, N., Polymeris, G.S., Loukou, Z., Kitis, G., 2006. Anomalous fading of the TL, Blue-SL and IR-SL signals of fluorapatite. Radiat. Meas. 41, 954–960.
Tsirliganis, N., Polymeris, G.S., Kitis, G., Pagonis, V., 2007. Dependence of the anomalous fading of the TL and blue OSL of fluorapatite on the occupancy of the tunnelling recombination sites. J. Lumin. 126, 303–308.
Tyler, S., McKeever, S.W.S., 1988. Anomalous fading of thermoluminescence in oligoclase. Nucl. Tracks Radiat. Meas. 14, 149–154.
Visocekas, R., Ceva, T., Marti, C., Lafaucheux, F., Roberts, M.C., 1976. Tunneling processes in afterglow of calcite. Phys. Stat. Sol. (a) 35, 315–327.
Visocekas, R., Geoffroy, A., 1977. Tunneling afterglows and retrapping in calcite. Phys. Stat. Sol. (a) 41, 499–503.
Visocekas, R., 1985. Tunneling radiative recombination in labradorite: its association with anomalous fading of thermoluminescence. Nucl. Tracks 10, 521–530.
Wintle, A.G., 1973. Anomalous fading of thermoluminescence in mineral samples. Nature 245, 143–144.
Wintle, A.G., 1977. Detailed study of minerals exhibiting anomalous fading. J. Lumin. 15, 385–393.